Biochemical and Biophysical Research Communications 450 (2014) 1095–1098

Contents lists available at ScienceDirect

Biochemical and Biophysical Research Communications

journal homepage: www.elsevier.com/locate/ybbrc

Serine phosphorylation on position 1033 of vinculin impacts cellular mechanics

Vera Auernheimer, Wolfgang H. Goldmann *

Department of Physics, Biophysics Group, Friedrich-Alexander-University Erlangen-Nuremberg, Germany

ARTICLE INFO

Article history:
Received 17 June 2014
Available online 1 July 2014

Keywords:
pS1033
Vinculin
Focal adhesions
Magnetic tweezer
Traction microscopy
FRAP

ABSTRACT

This study evaluates the influence of S1033 vinculin phosphorylation on the mechanical properties of cells. We demonstrate that MEFvcl KO cells transfected with the non-phosphorylatable eGFP-vinculin mutant S1033A are of lower stiffness compared to MEFvcl Rescue and phospho-mimicking mutant S1033D cells, which were of similar stiffness. Analogous, 2D traction microscopy indicates that MEFvcl Rescue and MEF mutant S1033D cells generate similar strain energy, but mutant S1033A cells display ~50% less strain energy. Fluorescence recovery after photobleaching demonstrates that the recovery time for mutant S1033A was significantly lower compared to MEFvcl Rescue and mutant S1033D and that the mobile fraction was smaller for MEFvcl Rescue and mutant S1033D than for mutant S1033A cells. This indicates that serine phosphorylation is required for the activation of vinculin and force transmission in focal adhesions.

1. Introduction

Vinculin phosphorylation is a potential mechanism for cellular focal adhesion growth and maturation. Five vinculin residues have been described as targets for phosphorylation by *src*-kinase [1] or protein kinase C (*PKC*) [2]: Y100, Y822, S1033, S1045, and Y1065 to potentially stabilize extracellular matrix (ECM) or cell–cell contacts [3,4]. These phosphorylation events are thought to be important for the formation of focal adhesions (FAs) and focal adherens junctions (FAJs) as well as cell signaling that could have biochemical, structural, and mechanical implications. For instance, cellular contacts induced through integrin binding to the ECM trigger signals into the cell and activate cellular vinculin. The FA complex, of which vinculin is an essential part, then grows and matures through mechano-induced scaffold formation and mechano-induced biochemical signal transduction [4–6]. The mode of action is understood for a number of structural and biochemical signals, thus an integrated mechanism by which the initial integrin-ECM contact develops into a mature focal adhesion is unknown. Upon integrin-ECM interaction, the scaffolding protein talin links integrin to F-actin filaments, constituting the initial focal contact [7]. Continued maturation, however, requires the force-induced recruitment of vinculin to the focal contact [8]. Understanding the mechanism and regulation of vinculin recruitment is therefore essential to explain the signaling dynamics by which focal adhesions are formed.

Vinculin is a binding partner for many FA proteins, and focal adhesion maturation is highly dependent on a process of vinculin activation, disrupting its head–tail interaction. Position Y100 and Y1065 [9,10] have been linked to *scr*-kinase phosphorylation, while S1033 and S1045 [11] were associated with PKC phosphorylation *in vitro*. Y822 has recently been described as a *src*-kinase phosphorylation target in adherens junctions [12]. Direct effects of mutating either S1033 or S1045 to a constitutive mimic of the phosphorylated or unphosphorylated form have not been tested, thus models have been put forward how their phosphorylation may affect vinculin recruitment [11]. Golji et al. [4] proposed in a simulation study that pY100 and pS1033 of vinculin are at the interface between the tail and head (D1) domain that could impact its activation and that phosphorylated vinculin requires less activating force to D1. In what way vinculin phosphorylation and maturing focal adhesions affect cellular force generation remained, however, open.

In this study, we analyzed vinculin's role as mechano-coupling protein using S1033 vinculin variants in magnetic tweezer and 2D-traction microscopic experiments. In additional experiments, we also determined the dynamics of vinculin variants measuring their recovery after photobleaching. The results suggest that force transmission is dependent on the phosphorylation of vinculin on position S1033, and that vinculin must be in an activated conformation incorporated in the focal adhesion complex to transmit forces *via* the actin network.

* Corresponding author.
E-mail address: wgoldmann@biomed.uni-erlangen.de (W.H. Goldmann).

http://dx.doi.org/10.1016/j.bbrc.2014.06.122
0006-291X/

2. Materials and methods

2.1. Cell culture

Wild-type (WT) and vinculin knock-out (KO) mouse embryonic fibroblasts (MEFs) were obtained from Dr. W.H. Ziegler [13]. These cell lines were maintained in a low glucose (1 g/L) Dulbecco's modified Eagle medium (Life Technologies, Darmstadt, Germany) supplemented with 10% fetal calf serum (low endotoxin) and 2 mM L-glutamine and kept at 37 °C with 5% CO_2. Mycoplasma contamination was excluded using a mycoplasma detection kit (Minerva Biolabs, Berlin, Germany).

2.2. Cloning and expression of vinculin

Generation of the eukaryotic expression vector pcDNA3.1, including eGFP-tagged wild-type vinculin was previously described by [14]. The same cDNA vector was used to obtain the serine mutants to analyze the phosphorylation effects. Using site-directed mutagenesis, serine on position 1033 was replaced by alanine (A) or aspartic acid (D).

To create point mutations, primers were ordered from MWG-Biotech (Eurofins MWG Operon, Ebersberg, Germany). Phusion High-Fidelity DNA Polymerase and the restriction enzyme DpnI for the digestion of methylated DNA were purchased from Cell Signaling (NEB, Frankfurt, Germany). DNA-vectors were amplified in *Escherichia coli* strain Dh5α and purified using the NucleoBond PC 500 kit (Macherey-Nagel, Düren, Germany). The complete sequence for all eGFP-tagged vinculin mutants was confirmed by sequencing (GATC Biotech AG, Konstanz, Germany). MEF cells (1.5×10^5) were seeded overnight in 35 mm cell culture dishes prior to transfection. Transfection was carried out in serum-free DMEM using 2 μg DNA and Lipofectamine 2000 (Invitrogen, Karlsruhe, Germany). The day after transfection, cells were re-seeded in 35 mm culture dishes or placed on PAA-traction gels, respectively.

2.3. Magnetic tweezer experiments

We used a magnetic tweezer device as described in [15]. For measurements, 3-4 $\times 10^4$ cells were seeded overnight into a 35 mm tissue culture dish. Thirty minutes before the experiment, the cells were incubated with fibronectin-coated paramagnetic beads of 4.5 μm ϕ (Invitrogen, Karlsruhe, Germany). A magnetic field was generated using a solenoid with a needle-shaped core (HyMu80 alloy, Carpenter, Reading, PA). The needle tip was placed at a distance of 20–30 μm from a bead bound to the cell using a motorized micromanipulator (Injectman NI-2, Eppendorf, Hamburg, Germany). A staircase-like, increasing force was then applied for 10 s to the bead bound on the cell surface [16,17]. During measurements, bright-field images were taken by a CCD camera (ORCA ER, Hamamatsu) at a rate of 40 frames/s. The bead position was tracked on-line using an intensity-weighted center-of-mass algorithm. Measurements on multiple beads per well were performed at 37 °C for 0.5 h, using a heated microscope stage on an inverted microscope at 40x magnification (NA 0.6) under bright-field illumination. Transfected MEFvcl KO cells were identified in fluorescence mode.

2.4. 2D-traction microscopy

Different MEFs were plated overnight on fibronectin-coated polyacrylamide hydrogels (Young's modulus of 18,000 Pa) at 37 °C and 5% CO_2 in DMEM medium. Gels were prepared according to a modified protocol by Pelham and Wang [18]. Using cytochalasin D and trypsin, cells were detached and images were recorded before and after relaxation of the gel. Comparing the position of fluorescent microspheres in the deformed and undeformed states, the traction field can be obtained using a difference-with-interpolation algorithm with a spatial resolution of 2.5 nm and an accuracy of 8 nm. Tractions were computed according to a Fourier-based-algorithm [19].

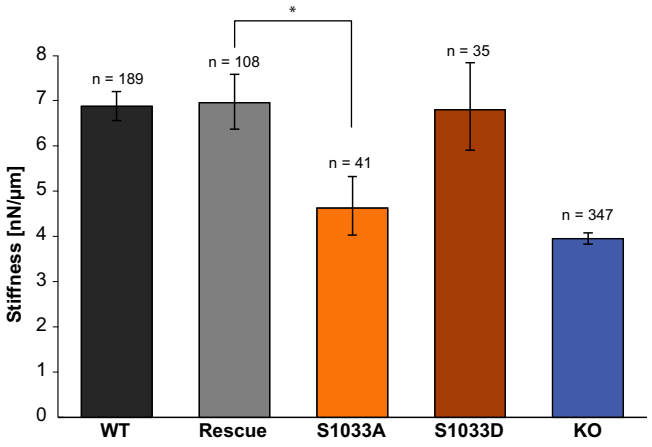

Fig. 2. Magnetic tweezer measurements at 6 nN force of MEFvcl WT (black), MEFvcl Rescue (gray), MEFvcl S1033A (orange), MEFvcl S1033D (red), and MEFvcl KO cells (blue). All cells were incubated with fibronectin-coated paramagnetic beads (Ø 4.5 μm) for 30 min, after which the paramagnetic beads were displaced from their original position by force application of the magnetic tweezer. MEFvcl WT, MEFvcl Rescue, and MEFvcl S1033D cells were by a factor ~1.6 stiffer than MEFvcl KO and MEFvcl S1033A cells. The standard error of the mean (SEM) and the number of cells analyzed per cell line are indicated by the bars. The asterisk indicates a significance level of $p < 0.05$. (For interpretation of the references to color in this figure legend, the reader is referred to the web version of this article.)

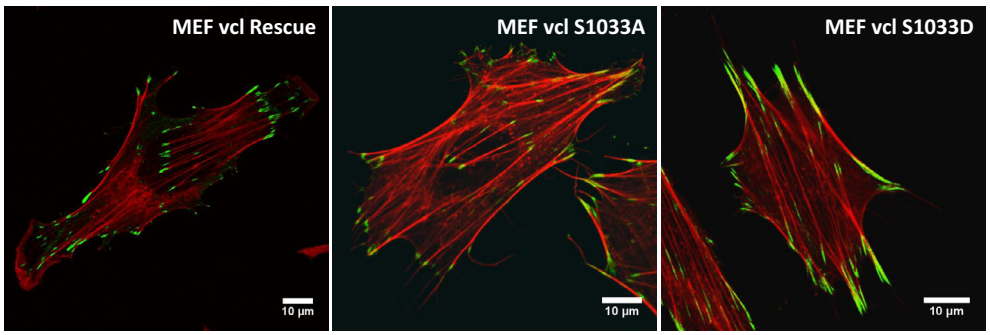

Fig. 1. Confocal images of MEFvcl KO cells transfected with eGFP-tagged vinculin (Rescue), S1033A, or S1033D mutant. Cells were seeded on fibronectin-coated glass slides overnight, fixed with 4% paraformaldehyde, and the actin cytoskeleton was stained with TRITC-phalloidin (Sigma–Aldrich, Taufkirchen, Germany). All vinculin constructs localized in the focal adhesions. Scale bars represent 10 μm.

2.5. Fluorescence recovery after photobleaching (FRAP)

FRAP studies were performed with the confocal microscope (Leica) and a 20× dip-in objective inside the incubation chamber. Transfected cells were cultivated in 35 mm dishes the day before, and cells expressing medium levels of eGFP-vinculin-constructs and focal adhesions that showed no growth or disassembly were chosen for measurements. A 488 nm argon laser was used for eGFP excitation and bleaching. Image acquisition started 1 min before bleaching and continued for 5 min of the recovery process (1 frame/4 s). FRAP movies were analyzed using ImageJ and Matlab software. Intensities of the bleached focal adhesions as well as reference adhesions were corrected for background fluorescence, and the bleached area was normalized by the average reference adhesion signal. Every recovery curve was fitted with a single exponential function, and the mean value of all half-life recovery times ($t_{1/2}$) as well as the immobile fractions were calculated.

3. Results and discussion

In this study, we mutated serine on position 1033 of the vinculin molecule to alanine (A, non-phosphorylatable) and to aspartic acid (D, phospho-mimicking) to test the cell mechanical changes induced by phosphorylation. Both vinculin constructs were expressed in MEFvcl KO cells, and they located in the focal adhesions regularly (Fig. 1). We measured the cell stiffness of MEF vinculin variants using the magnetic tweezer device and observed that wildtype, rescue, and mutant S1033D cells at 6 nN force exhibited similar stiffness of around 7 nN/μm, while MEFvcl KO and mutant S1033A showed significantly lower stiffness (Fig. 2). These results support the hypothesis that phosphorylation of vinculin on position 1033 is necessary for protein activation and binding to actin [4].

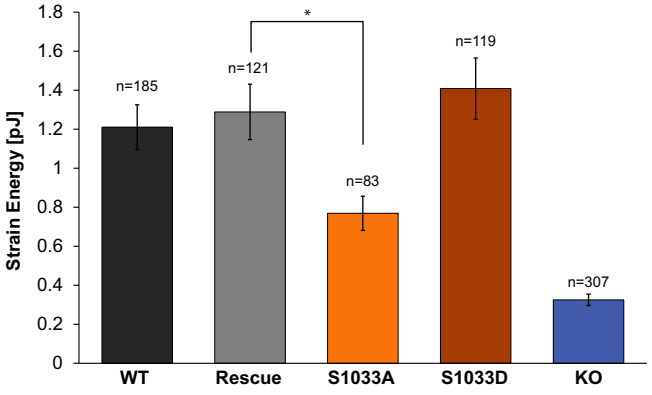

Fig. 3. 2D traction microscopy of MEFvcl WT, MEFvcl Rescue, MEFvcl S1033A, MEFvcl S1033D, and MEFvcl KO cells. All cells were seeded on fibronectin-coated elastic substrates (~18 kPa) and tractions were determined. The strain energy values of MEFvcl WT, MEFvcl Rescue, and MEFvcl S1033D cells were ~4 fold higher than MEFvcl KO cells and ~1.6-fold higher than MEFvcl S1033A cells. The standard error of the mean (SEM) is indicated by the bars; the number of cells analyzed per cell line were $n \geqslant 83$. The asterisk indicates a significance level of $p < 0.05$.

Two-dimensional traction microscopic measurements further support this view. We could demonstrate that the contractile forces generated *via* the intracellular integrin-FA-actomyosin link are markedly higher in MEFvcl WT, MEFvcl Rescue, and S1033D mutant cells compared to MEFvcl S1033A mutant and MEFvcl KO cells (Fig. 3). We, therefore, believe that phosphorylation of vinculin is necessary for its force transmission function.

Since the dynamics of focal adhesion proteins are linked to focal adhesion assembly/disassembly and consequently to force generation [20,21], we also determined the exchange rates of vinculin within focal adhesions using the FRAP technique. The exchange rate of vinculin in focal adhesions was measured in MEFvcl KO cells re-expressing intact vinculin (Rescue), or S1033D, or S1033A vinculin mutants. The half-maximum recovery time after photobleaching ($t_{1/2}$) of vinculin fused with eGFP was quantified (Fig. 4A). Vinculin exchange dynamics in rescue cells ($t_{1/2} = 67 \pm 8$ s) and in cells re-expressing the vinculin mutant S1033D ($t_{1/2} = 70 \pm 16$ s) were significantly slower compared to cells expressing the vinculin mutant S1033A ($t_{1/2} = 42 \pm 6$ s). These results indicate that the non-phosphorylatable mutant (S1033A) increases the exchange dynamics in focal adhesions and reduces the stability of vinculin incorporation, which is also indicated from the ratio of the mobile/immobile fraction of the vinculin variants (Fig. 4B). The immobile fraction increases for the constitutively phospho-mimicking mutant S1033D. These results imply that phosphorylation probably primes the protein and increases the affinity to certain vinculin binding partners, allowing for force activation.

This was previously suggested by Golji et al. [4] from simulation studies. These researchers proposed that (i) local conformational changes induced through phosphorylation of vinculin at position S1033 could facilitate vinculin activation by destabilizing the autoinhibiting head-tail-interaction, and (ii) cooperative binding events involving actin and talin with the resulting force generation

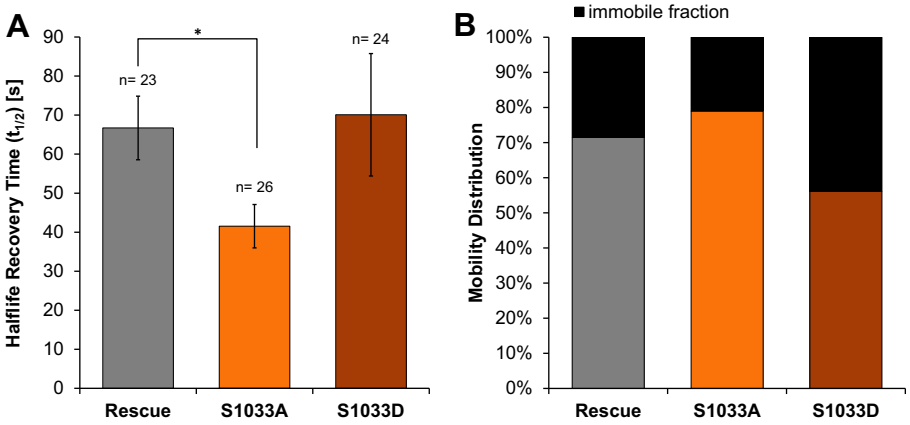

Fig. 4. Dynamics of vinculin variants measured by FRAP. (A) The bar plot shows half-life recovery times of eGFP-fused vcl Rescue, vcl S1033A, and vcl S1033D in MEF cells. The standard error of the mean (SEM) is indicated by the bars; the number of cells analyzed per cell line were between 23 and 26 cells. The asterisk indicates a significance level of $p < 0.05$. (B) Plot of the mobile/immobile fraction of vinculin variants in focal adhesions. Mobile fractions are indicated in color and immobile fractions are represented in black. (For interpretation of the references to color in this figure legend, the reader is referred to the web version of this article.)

would probably still be necessary. They hypothesized that the phosphorylation of S1033 could affect the interface between vinculin tail and vinculin head domain (D1), what could be an effective contribution of vinculin activation and focal adhesion formation. But it is still unknown, if phosphorylation at S1033 actually plays any role in physiological processes *in vivo*. Ziegler at al. [11] had previously suggested that S1033 vinculin needs to be recruited to the submembranous location to become phosphorylated by PKC. Lipid membrane attachment or insertion of vinculin tail and phosphorylation at Y1065 by *src*-kinase have also been proposed by others [1,22,23] to support vinculin activation. Although we are unsure in which order the different factors are involved in vinculin activation and stabilization, we believe that serine phosphorylation is a prerequisite for proper vinculin function in the cell.

Acknowledgments

We thank Ms. Sinja-Fee Schramm for technical help and Drs. Ingo Thievessen and Ben Fabry for stimulating discussions. This work was supported by grants from Deutscher Akademischer Austausch Dienst and Deutsche Forschungsgemeinschaft.

References

[1] N.Q. Balaban, U.S. Schwarz, D. Riveline, P. Goichberg, G. Tzur, I. Sabanay, D. Mahalu, S. Safran, A. Bershadsky, L. Addadi, B. Geiger, Force and focal adhesion assembly: a close relationship studied using elastic micropatterned substrates, Nat. Cell Biol. 3 (2001) 466–472.
[2] D.K. Werth, J.E. Niedel, I. Pastan, Vinculin, a cytoskeletal substrate of protein kinase-C, J. Biol. Chem. 258 (1983) 1423–1426.
[3] X. Peng, E.S. Nelson, J.L. Maiers, K.A. DeMali, New insights into vinculin function and regulation, Int. Rev. Cell Mol. Biol. 287 (2011) 191–231.
[4] J. Golji, T. Wendorff, M.R. Mofrad, Phosphorylation primes vinculin for activation, Biophys. J. 102 (2012) 2022–2030.
[5] J. Golji, M.R. Mofrad, A molecular dynamics investigation of vinculin activation, Biophys. J. 99 (2010) 1073–1081.
[6] J. Golji, J. Lam, M.R. Mofrad, Vinculin activation is necessary for complete talin binding, Biophys. J. 100 (2011) 332–340.
[7] C.S. Izzard, A precursor of the focal contact in cultured fibroblasts, Cell Motil. Cytoskeleton 10 (1988) 137–142.
[8] C. Möhl, N. Kirchgessner, C. Schäfer, K. Küpper, S. Born, G. Diez, W.H. Goldmann, R. Merkel, B. Hoffmann, Becoming stable and strong: the interplay between vinculin exchange dynamics and adhesion strength during adhesion site maturation, Cell Motil. Cytoskeleton 66 (2009) 350–364.
[9] Z. Zhang, G. Izaguirre, S.Y. Lin, H.Y. Lee, E. Schaefer, B. Haimovich, The phosphorylation of vinculin on tyrosine residues 100 and 1065, mediated by SRC kinases, affects cell spreading, Mol. Biol. Cell 15 (2004) 4234–4247.
[10] S. Moese, M. Selbach, V. Brinkmann, A. Karlas, B. Haimovich, S. Backert, T.F. Meyer, The *Helicobacter pylori* CagA protein disrupts matrix adhesion of gastric epithelial cells by dephosphorylation of vinculin, Cell. Microbiol. 9 (2007) 1148–1161.
[11] W.H. Ziegler, U. Tigges, A. Zieseniss, B.M. Jockusch, A lipid-regulated docking site on vinculin for protein kinase C, J. Biol. Chem. 277 (2002) 7396–7404.
[12] K.A. DeMali, Vinculin-a dynamic regulator of cell adhesion, Trends Biochem. Sci. 29 (2004) 565–567.
[13] C.T. Mierke, P. Kollmannsberger, D.P. Zitterbart, G. Diez, T.M. Koch, S. Marg, W.H. Ziegler, W.H. Goldmann, B. Fabry, Vinculin facilitates cell invasion into three-dimensional collagen matrices, J. Biol. Chem. 285 (2010) 13121–13130.
[14] G. Diez, V. Auernheimer, B. Fabry, W.H. Goldmann, Head/tail interaction of vinculin influences cell mechanical behavior, Biochem. Biophys. Res. Commun. 406 (2011) 85–88.
[15] P. Kollmannsberger, B. Fabry, High-force magnetic tweezers with force feedback for biological applications, Rev. Sci. Instrum. 78 (2007) 114301–114306.
[16] F.J. Alenghat, B. Fabry, K.Y. Tsai, W.H. Goldmann, D.E. Ingber, Analysis of cell mechanics in single vinculin-deficient cells using a magnetic tweezer, Biochem. Biophys. Res. Commun. 277 (2000) 93–99.
[17] C.T. Mierke, P. Kollmannsberger, D. Paranhos-Zitterbart, J. Smith, B. Fabry, W.H. Goldmann, Mechano-coupling and regulation of contractility by the vinculin tail domain, Biophys. J. 94 (2008) 661–670.
[18] R.J. Pelham Jr., Y. Wang, Cell locomotion and focal adhesions are regulated by substrate flexibility, Proc. Natl. Acad. Sci. U.S.A. 94 (1997) 13661–13665.
[19] J.P. Butler, I.M. Tolic-Norrelykke, B. Fabry, J.J. Fredberg, Traction fields, moments, and strain energy that cells exert on their surroundings, Am. J. Physiol. Cell Physiol. 282 (2002) C595–C605.
[20] R. Janostiak, J. Brabek, V. Auernheimer, Z. Tatarova, L.A. Lautscham, T. Dey, J. Gemperle, R. Merkel, W.H. Goldmann, B. Fabry, D. Rosel, CAS directly interacts with vinculin to control mechanosensing and focal adhesion dynamics, Cell. Mol. Life Sci. 71 (2014) 727–744.
[21] K. Küpper, N. Lang, C. Möhl, N. Kirchgessner, S. Born, W.H. Goldmann, R. Merkel, B. Hoffmann, Tyrosine phosphorylation of vinculin at position 1065 modifies focal adhesion dynamics and cell tractions, Biochem. Biophys. Res. Commun. 399 (2010) 560–564.
[22] G. Diez, P. Kollmannsberger, C.T. Mierke, T.M. Koch, H. Vali, B. Fabry, W.H. Goldmann, Anchorage of vinculin to lipid membranes influences cell mechanical properties, Biophys. J. 97 (2009) 3105–3112.
[23] V.F. Wirth, F. List, G. Diez, W.H. Goldmann, Vinculin's C-terminal region facilitates phospholipid membrane insertion, Biochem. Biophys. Res. Commun. 398 (2010) 433–437.